Materials Research Proceedings 37 (2023) 202-205 https://doi.org/10.21741/9781644902813-44

Thermal fluid-structure interaction by discontinuous Galerkin methods

Vincenzo Gulizzi[1,a*]

[1]Department of Engineering, University of Palermo, Viale delle Scienze, 90128, Palermo

[a]vincenzo.gulizzi@unipa.it

Keywords: Thermal Fluid-Structure Interaction, Discontinuous Galerkin Methods, High-Order Accuracy

Abstract. This research study presents a novel high-order accurate computational framework for thermal fluid-structure interaction problems. The framework is based on the use of block-structured Cartesian grids where level set functions are employed to define both the fluid and the solid regions. This leads to a mesh that consists of a collection of standard *d*-dimensional rectangular elements and a relatively smaller number of irregular elements at the fluid-solid interface. The embedded boundaries are resolved with high-order accuracy thanks to the use of high-order accurate quadrature rules for implicitly-defined regions. The fluid is assumed compressible and governed by the inviscid Navier-Stokes equations, whilst the solid region obeys the equations of thermo-elasticity within the small-strain regime. Numerical examples are provided to assess the capability of the proposed approach.

Introduction

The interest in developing reliable, sustainable and reusable transportation systems that are capable of flying at Mach numbers ranging from 0 to 12 is continuously growing. It is well-known that, within such a wide flight regime, the aircraft structure must endure extreme conditions in terms of pressure and temperature loads. These loads induce a complex thermo-elastic interaction that is generally resolved via the aid of numerical methods as analytical solutions exist for very special combinations of boundary conditions and material properties.

In the context of computational methods, the Finite Volume (FV) method is the industry-standard numerical approach to fluid mechanics problems and is found in many open-source and commercial software libraries; on the other hand, thermo-mechanical problems are very often tackled by the Finite Element (FE) method. Both the FV and the FE methods are extremely robust and widely employed in science and engineering; however, their coupling may become involved and may represent the bottleneck for fluid-structure interaction simulations.

Among the various alternatives to FV- or FE-based approaches, the discontinuous Galerkin (DG) method has proved a powerful numerical technique for both fluid- and solid-mechanics; see, e.g., [1], among several recent contributions. With respect to other techniques, DG-based formulations use spaces of discontinuous basis functions to approximate the solution fields; this naturally enables high-order accuracy with generally shaped mesh elements, block-structured mass matrices and massive parallelization. Additionally, as DG methods enforce both boundary and interface conditions in a weak sense, the coupling between different formulations for the same or for different sets of partial differential equations is significantly simplified. This includes the coupling between different DG formulations or between a DG formulation and a FVM scheme, see Ref.[2].

This study introduces a novel formulation for unsteady thermal fluid-structure interaction problems coupling a shock-capturing FV scheme and a high-order DG scheme. Numerical tests are presented for a thermo-elastic cylinder moving at supersonic speed in an inviscid gas.

Materials Research Proceedings 37 (2023) 202-205 https://doi.org/10.21741/9781644902813-44

Geometry representation and discretization

The coupled thermal fluid-structure interaction problem involves the modeling of two regions consisting of a fluid domain and a solid domain. Here, the geometry is represented via a level set function φ defined in a rectangular domain $\mathcal{R} \subset \mathbb{R}^d$, such that the fluid domain $\mathcal{D}^g$ and the solid domain $\mathcal{D}^s$ are identified by the points belonging to $\mathcal{R}$ where φ is negative and where φ is positive, respectively. It follows that the interface $\mathcal{J}$ between the fluid and the solid domains is identified by $\{\boldsymbol{x} \in \mathcal{R} : \varphi(x) = 0\}$. To illustrate, Fig.(1a) shows a level set function defining a circle in a square domain, whilst Fig.(1b) shows the corresponding fluid and solid regions.

The fluid and the solid domains are eventually discretized. Here, we use the implicitly-defined mesh approach developed in Refs.[2,3,4], which is based on intersecting a structured grid with the zero-contour of the level set functions and allows resolving the curved boundaries with high-order accuracy. Fig.(1c) shows the implicitly defined mesh for the geometry shown in Fig.(1b); in the figure, the darker elements represent the extended elements that prevent the presence of overly small elements in the mesh. See Refs.[2,3,4] for further detail on this meshing strategy.

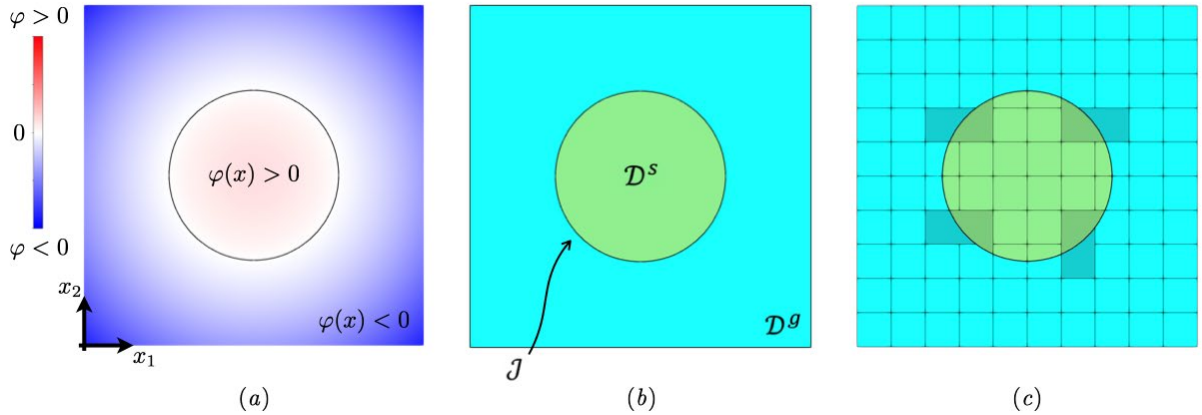

Fig. 1: (a). Level set function defined in a two-dimensional square and (b) corresponding fluid and solid regions identified by the sign of the level set function. (c) Implicitly defined mesh.

Fluid dynamics model

The considered fluid is a compressible gas assumed to obey the Euler equations, which are expressed as the following conservation law:

$$\frac{\partial \boldsymbol{U}^g}{\partial t} + \frac{\partial \boldsymbol{F}_k^g}{\partial x_k} = 0, \tag{1}$$

where t is time, x_k is the k-th spatial component, and $\boldsymbol{U}^g$ and $\boldsymbol{F}_k^g$ denote the $(d+2)$-dimensional vectors of the conserved variables and the flux in the k-th direction, respectively; these are

$$\boldsymbol{U}^g \equiv \begin{pmatrix} \rho^g \\ \rho^g \boldsymbol{v}^g \\ \rho^g e_0 \end{pmatrix} \quad \text{and} \quad \boldsymbol{F}_k^g \equiv \begin{pmatrix} \rho^g v_k^g \\ \rho^g v_k^g \boldsymbol{v}^g + p\boldsymbol{\delta}_k \\ (\rho^g e_0 + p) v_k^g \end{pmatrix}, \tag{2}$$

where ρ^g is the fluid density, $\boldsymbol{v}^g \equiv \left(v_1^g, \ldots, v_d^g\right)^{\mathrm{T}}$ is the gas velocity vector, e_0 is the gas total energy and p is the gas pressure. The governing equations are closed by the ideal-gas equation of state with ratio γ of specific heats. In Eq.(1) and in the remainder of the paper, Latin indices will take value in $\{1,\ldots,d\}$ and, when repeated, imply summation.

Materials Research Proceedings 37 (2023) 202-205 https://doi.org/10.21741/9781644902813-44

Thermo-mechanical model

The thermo-mechanical model considered here is based on the theory of linear elasticity and Fourier's law of heat conduction. In absence of external sources, it is possible to show that the governing equations of coupled, unsteady thermo-elasticity may be written as:

$$\frac{\partial \boldsymbol{U}^s}{\partial t} - \frac{\partial}{\partial x_k}\left(\boldsymbol{Q}_{kl}\frac{\partial \boldsymbol{U}^s}{\partial x_l} + \boldsymbol{R}_k \boldsymbol{U}^s\right) + \boldsymbol{R}_k^* \frac{\partial \boldsymbol{U}^s}{\partial x_k} + \boldsymbol{S}\boldsymbol{U}^s = \boldsymbol{0}, \tag{3}$$

where

$$\boldsymbol{U}^s \equiv \begin{pmatrix} \boldsymbol{u}^s \\ \boldsymbol{v}^s \\ \vartheta \end{pmatrix}, \quad \boldsymbol{Q}_{kl} \equiv \begin{pmatrix} \boldsymbol{0} & \boldsymbol{0} & \boldsymbol{0} \\ \frac{\boldsymbol{c}_{kl}}{\rho^s} & \boldsymbol{0} & \boldsymbol{0} \\ \boldsymbol{0} & \boldsymbol{0} & \frac{\kappa_{kl}}{c^s} \end{pmatrix}, \quad \boldsymbol{R}_k \equiv \begin{pmatrix} \boldsymbol{0} & \boldsymbol{0} & \boldsymbol{0} \\ \boldsymbol{0} & \boldsymbol{0} & -\frac{\boldsymbol{m}_k}{\rho^s} \\ \boldsymbol{0} & \boldsymbol{0} & 0 \end{pmatrix}, \quad \boldsymbol{R}_k^* \equiv \begin{pmatrix} \boldsymbol{0} & \boldsymbol{0} & \boldsymbol{0} \\ \boldsymbol{0} & \boldsymbol{0} & \boldsymbol{0} \\ \boldsymbol{0} & \frac{T_0\,\boldsymbol{m}_k^{\mathrm{T}}}{c^s} & 0 \end{pmatrix} \tag{4a}$$

and

$$\boldsymbol{S} \equiv \begin{pmatrix} \boldsymbol{0} & -\mathbf{I}_d & \boldsymbol{0} \\ \boldsymbol{0} & \boldsymbol{0} & \boldsymbol{0} \\ \boldsymbol{0} & \boldsymbol{0} & 0 \end{pmatrix}. \tag{4b}$$

In Eq.(4), $\boldsymbol{u}^s \equiv (u_1^s, \dots, u_d^s)^{\mathrm{T}}$ is the solid displacement vector, $\boldsymbol{v}^s \equiv (v_1^s, \dots, v_d^s)^{\mathrm{T}}$ is the solid velocity vector, $\vartheta \equiv T^s - T_0$ represents the variation of the solid temperature field T^s with respect to a reference temperature T_0, ρ^s and c^s are the density and the heat capacity per unit volume, respectively, of the solid domain, $\boldsymbol{c}_{kl}$ is a $d \times d$ matrix collecting subsets of elastic coefficients, see, e.g., Refs.[5], κ_{kl} is the kl-th entry of thermal conductivity tensor, $\boldsymbol{m}_k$ is the d-dimensional vector containing components of the thermo-elasticity tensor, and $\mathbf{I}_d$ is the $d \times d$ identity matrix. It is noted that the thermo-elastic properties of the solid are assumed temperature independent.

Thermal fluid-structure coupling

The coupling between the gas region and the solid region occurs at the interface between the two domains, i.e. at $\mathcal{J}$ shown in Fig.(1b). Recalling that the solid is assumed to undergo small deformations, its interface with the gas do not change with time and, as such, behaves like a fixed wall for the gas dynamics equations. Additionally, as the gas is assumed inviscid and non-conducting, its temperature T^g is determined by the equation of state.

The thermal fluid-structure coupling problem is then solved as follows: the conserved variables of Eq.(1) are updated from the time instant t to the time instant $t + \mathrm{d}t$ using an explicit time-integration algorithm; then, at the time $t + \mathrm{d}t$, the computed values of the gas pressure and temperature provide the required boundary conditions at the gas-solid interface to solve the unsteady thermo-elastic problem.

Discontinuous Galerkin formulation

The governing equations of the gas domain, i.e. Eq.(1), are numerically solved via the time-explicit Runge-Kutta discontinuous Galerkin formulation coupled to a shock-capturing second-order FV scheme [2,4]. On the other hand, the equations governing the thermo-elastic solid are solved by extending the DG formulation for elliptic PDEs developed in Refs.[5] with suitably-defined terms accounting for the temporal derivatives in Eq.(3). See Ref.[6] for further detail.

Results

Numerical results are presented for a cylinder with radius $\boldsymbol{r} = \boldsymbol{0.2}$ m moving at a Mach number $\mathbf{M}_\infty = \boldsymbol{2}$ at an altitude $\boldsymbol{h} = \boldsymbol{10}$ km; the geometry and the boundary conditions of the problem are sketched in Fig.(2a). The final time of simulation is $\boldsymbol{I_t} = \boldsymbol{3}$ ms. The gas is assumed perfect with $\boldsymbol{\gamma} = \boldsymbol{1.4}$, while the solid is assumed isotropic with properties: density 2700 kg/m^3, Young's

modulus 70 GPa, Poisson's ratio 0.33, thermal conductivity coefficient 210 W/(m K), thermal expansion coefficient $\mathbf{24} \times \mathbf{10^{-6}}$ 1/K and volumetric heat capacity $\mathbf{2.43} \times \mathbf{10^{6}}$ J/(m^3 K).

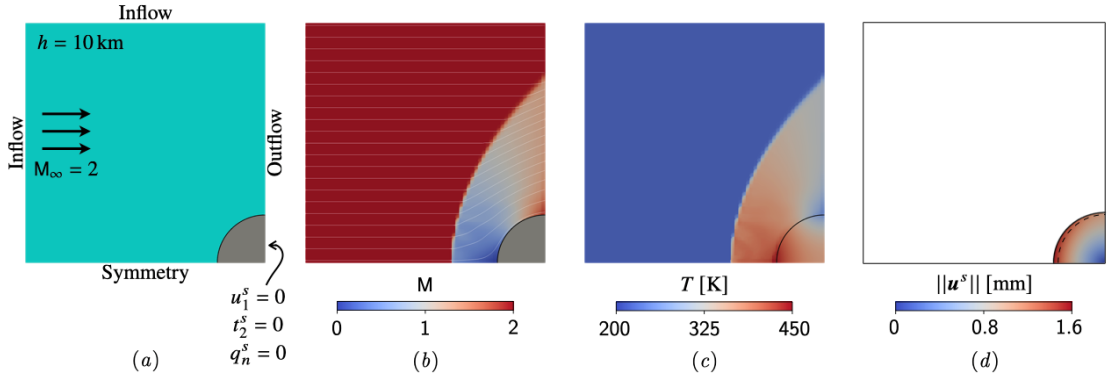

Fig. 2: (a) Geometry and boundary conditions. (b) Mach number. (c) Temperature. (d) Displacement magnitude (the dashed line denotes the undeformed shape).

Fig.(2b) shows the distribution of the Mach number, Fig.(2c) shows the temperature distribution within both the gas and the solid, while Fig.(2d) shows the displacement magnitude of the solid. The figures confirm the ability of the formulation to capture the shock wave, the thermal loads induced by the fluid flow and the deformation of the body.

Conclusions

A novel formulation for unsteady thermal fluid-structure interaction problems has been presented. The formulation uses a high-order accurate represented of embedded geometries, a shock-capturing FV scheme to resolve flow discontinuities, and a high-order accurate DG scheme for the thermo-elastic problem. Numerical results have been presented for a thermo-elastic cylinder moving at $\mathrm{M} = 2$ and have showed the capability of the proposed approach.

References

[1] Z.Cai and B. Thornber. A high-order discontinuous Galerkin method for simulating incompressible fluid-thermal-structural interaction problems. International Journal of Heat and Fluid Flow, 83 (2020), p.108572. https://doi.org/10.1016/j.ijheatfluidflow.2020.108572

[2] V. Gulizzi, A.S. Almgren and J.B. Bell. A coupled discontinuous Galerkin-Finite Volume framework for solving gas dynamics over embedded geometries. Journal of Computational Physics, 450 (2022), p.110861. https://doi.org/10.1016/j.jcp.2021.110861

[3] R. Saye. Implicit mesh discontinuous Galerkin methods and interfacial gauge methods for high-order accurate interface dynamics, with applications to surface tension dynamics, rigid body fluid–structure interaction, and free surface flow: Part I. Journal of Computational Physics, 344 (2017), pp.647-682. https://doi.org/10.1016/j.jcp.2017.04.076

[4] V. Gulizzi and R. Saye. Modeling wave propagation in elastic solids via high-order accurate implicit-mesh discontinuous Galerkin methods. Computer Methods in Applied Mechanics and Engineering, 395 (2022), 114971. https://doi.org/10.1016/j.cma.2022.114971

[5] V. Gulizzi, I. Benedetti and A. Milazzo. A high-resolution layer-wise discontinuous Galerkin formulation for multilayered composite plates. Composite Structures, 242 (2020), 112137. https://doi.org/10.1016/j.compstruct.2020.112137

[6] V. Gulizzi, I. Benedetti and A. Milazzo. Discontinuous Galerkin Methods for Solids and Structures. in: M.H. Ferri Aliabadi, W.O. Soboyejo (Eds.), Comprehensive Structural Integrity 2nd edition, Oxford: Elsevier, 2023, pp. 348-377. https://doi.org/10.1016/B978-0-12-822944-6.00024-4